Short Communication

Corrosion Behavior of the AA2124 Aluminium Alloy Exposed to Ethanol Mixtures

W. Aperador[1*], J. Caballero-Gómez[1], A. Delgado[1,2].

[1] Departament of Engineering, Universidad Militar Nueva Granada, Carrera 11 No. 101-80,
Fax:+57(1) 6343200, Bogotá, Colombia.
[2] Escuela Colombiana de Ingeniería Julio Garavito. Bogotá, Colombia.
[*]E-mail: g.ing.materiales@gmail.com

In the present article was studied the corrosion behavior of the AA2124 aluminum alloy which is a material used to fabricate parts of combustion engines, in a gasoline-bioethanol mixtures with concentrations of 5%, 10% and 20%. The evaluation was performed by potentiodynamics techniques and electrochemical impedance spectroscopy. It was determinate that the corrosion is more evident for mixtures with a greater amount of bioethanol and the corrosion type generated was superficial that begins on a clean surface and extends below it.

1. INTRODUCTION

The increase of the vehicles fleet year by year in the world has generated a direct relation with the environmental contamination by the greenhouse gas constant emissions. Furthermore, the variability in oil prices has shown a clear need for new opportunities of fuel generating based on renewable resources; currently, the implementation of biofuel is given in some countries with small plants producing of bioethanol of crude sugar origin, which has been established for a mixture of 10% bioethanol with gasoline from fossil origin. This scenario has motivated an incessant search of solutions to the energetic problem. The answers aim to the possible substitution of the petroleum fuels by cleaner fuel; such as the biofuels of vegetal or animal origin. [1-4].

The bioethanol has some attributes that place it in advantage front the gasoline from fossil origin, some of these are: decreasing the greenhouse effect caused by the increase in pollutants as CO_2 in the atmosphere, aromatic, not toxic and biodegradable. Its utilization reduce notoriously the exhaust

gases, moreover acts as a fuel additive. The bioethanol utilization in mixtures with gasoline in an engine up to 20% in volume does not require modifications in Otto cycle engines; for greater bioethanol proportion is require modifications in the engines designs. [5-6].

The production of bioethanol is performed with commercial bases, using sweet source materials, directly fermentable, such as the sugarcane. From the economic viewpoint, the opportunity cost analysis of the sugarcane bioethanol front to the sugar and the molasses, and the comparison of prices paid to producers of bioethanol [7-10].

The aim of this work is studying the effect of the bioethanol mixture percentage on the obtention of alternative fuel for gasoline engines; the work was performed in two phases, in the first phase was obtained the bioethanol and gasoline mixture, subsequently in the second phase were performed electrochemical tests to evaluate the behavior of the biofuel at 5%, 10% and 20% of bioethanol in the mixtures, in contact with the AA2124 alloy.

2. MATERIALS AND METHODS

2.1 Materials

The chemical composition of the evaluated alloy was determinate by X ray fluorescence (XRF) of dispersive energies using a spectrometer Philips model PW-1480, Sc/Mo anode, generator tension of 80 kV and current of 35mA.

Table 1. Chemical composition of the AA2124 aluminum alloy.

Alloy	% Cu	% Mg	% Mn	% Fe	% Si	% Cr	% Zn	% Al
AA2124	4.31	1.29	0.81	0.19	0.07	0.08	0.07	93.18

The fuels used were 100% regular gasoline and gasoline mixtures of regular and bioethanol at 5%, 10% and 20% percentage.

2.2 Evaluation techniques

For the corrosion resistance evaluation in static condition was used a potentiostat – galvanostat, Gamry PCI-4 model. It was used electrochemical impedance spectroscopy (EIS) and anodic polarization curves techniques. The electrochemical corrosion test was performed at a temperature of $25\pm0.2°C$, using as electrolyte the bioethanol-gasoline mixtures, all the tests were done in duplicate. For the assembly was used a cell composed by a platinum counter electrode, an Ag/AgCl reference electrode and as a working electrode the aluminum alloys with an exposed area of $1cm^2$. The samples to evaluate were polish previously until getting a low rugosity surface, which was done with an abrasive paper of increasing size of SiC, from 100 to 0.05 μm in a gyratory disc. The Nyquist diagrams were obtained by frequency sweeps in the range of 0.001 Hz to 100 kHz, using sinusoidal signal

amplitude of 10 mV. The polarization curves were measured after one hour of immersion, with a sweep velocity of 1 mV/s, in a voltage range from -250 mV to +1250 mV with respect to the corrosion potential (Ecorr). The corrosion velocity values (Vcorr) were calculated from the Tafel pending and the value of the corrosion current (Icorr) in a potential range of ±250 mV vs. Ecorr, from the anodic polarization curves.

The superficial characteristics were determinate with a scanning electronic microscopy (SEM) JEOL 5000 that works in a magnification range of 10-40000X and a high sensibility detector (multi-mode) for retro-dispersed electrons. The SEM technique allowed the microstructural study subsequent to the potentiodynamic evaluation.

3. RESULTS

3.1 Potentiodynamic curve

The figure 1 shows the potentiodynamic curves for the tested aluminum alloy evaluated in different electrolytes (regular gasoline 100% and mixtures of regular gasoline and bioethanol with percentages of 5%, 10% and 20%). In the polarization curve obtained by the exposition of the aluminum to different electrolytes, it was observed the uninterrupted progress of the anodic branch when the working potential increase, which provides a clear indication of the progress of general corrosion on the surface according to what is shown in the figure 1. In turn, it is observed that the polarization curve displaces the point of intersection of the branches anodic and cathodic (Icorr, Ecorr) to more active potentials and greater current densities, in comparison with the observed by exposing the material to percentages of 10 and 20%; it means that the material will present the general corrosion phenomenon with greater spontaneity and greater kinetic or evolution of corrosive process, due to the ethanol being hygroscopic absorbs more water, which accelerates corrosion processes [11].
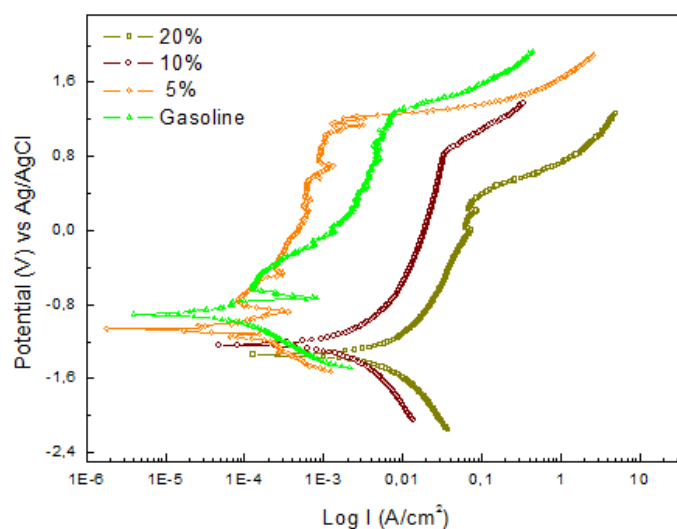

Figure 1. Anodic polarization curves of the corrosion behavior of the AA 2124 immersed in gasoline mixtures of regular and bioethanol at 5%, 10% and 20% percentage.

The rest potential showed in the table 2 and obtained by the potentiodynamics curves, provide an approach to the thermodynamic behavior of the alloy AA2124 against corrosive phenomenon once interacts with the electrolyte, in which case is observed for the medium 20% bioethanol-gasoline that the alloy is more active follow by 10% bioethanol-gasoline, 5% bioethanol-gasoline and finally the gasoline [12].

The results of corrosion current and corrosion velocity can be analysis in group in the figure 1 and table 2, respectively given the intrinsic relation that exist between the variables. Such as is observed in the graphics above the bioethanol at 20% presents the lowest progress of the corrosive phenomenon behavior follow by the bioethanol at 10%, the behavior improves when the bioethanol at 5% is evaluated. In the Tafel diagrams all the aluminum alloys show an increase of the current density by increasing the potential in the anode region; this is owing to in the studied material is presented pitting corrosion, which generates an increased in the corrosion velocity. The pitting corrosion is more progressive when the attacked area is small generating a higher depth in the pitting due to the formation of differential aeration cell, where the base of de pitting performs more anodically and the pH decreases making difficult the formation of coatings.

Table 2. Values of electrochemical parameters for AA 2124, obtained from polarization curves in the corrosion system.

	Corrosion Potencial (mV)	Corrosion Current ($\mu A/cm^2$)	Corrosion rate (μmy)
20% Bioethanol	-1340	5.77	3.28
10% Bioethanol	-1239	1.55	1.05
5% Bioethanol	-1073	0.12	0.063
Regular gasoline	-888	0.091	0.059

3.2 EIS Measurements

In the figure 3 is observed the impedance spectrums; the superiority in the electrochemical behavior at low frequencies of the regular gasoline and the bioethanol at 5% excels in relation to the polarization resistance, which can be attributed to its thermodynamic stability by effect of the reduction in the water content and the capability of passivation which has the evaluated substratum (alumina layer). On the other hand, the bioethanol at 20% has the lowest polarization resistance, while the bioethanol at 10% is located in intermediate. It is important to note that for the studied aluminum alloy; furthermore it was doped with Cr, and Mg, which presents a thermal treatment of aging that, seeks hardening the material by the precipitates generating coherent with the matrix so as to obtain the best properties in service; this thermal treatment has important implications from the thermodynamic viewpoint over the electrochemical behavior of the material, since a structure out of balance has higher reaction potential with the medium as well as encouraging localized attack phenomenon. On the other

hand, in this electrochemical cell exists an electric resistance as well, associated to de electrolyte resistance (Rs) that will be equally evident in the total impedance of the system.
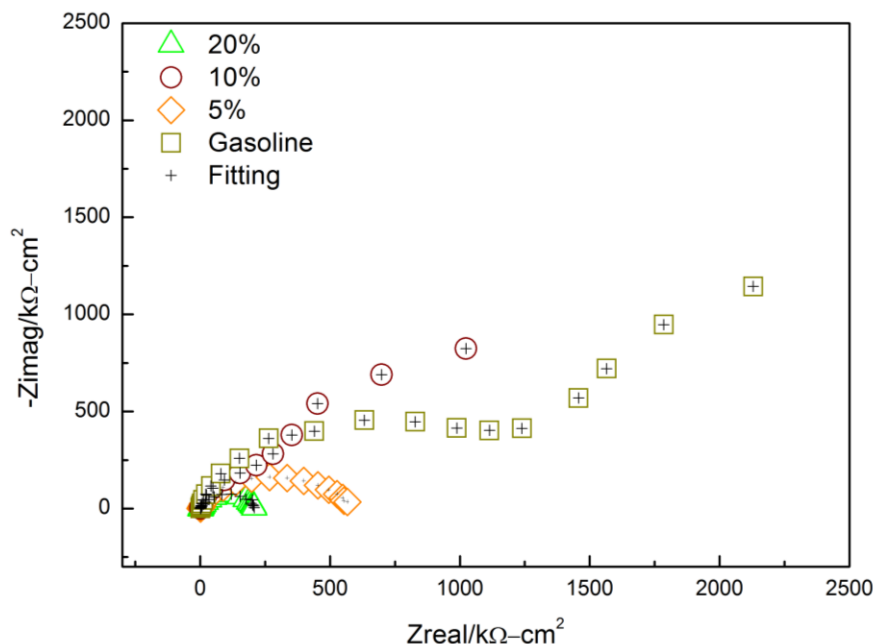

Figure 3. Impedance diagrams of corrosion for AA 2124 immersed in gasoline mixtures of regular and bioethanol at 5%, 10% and 20% percentage.

The degradation which occurs bioethanol has been studied in other industrial materials [13-14]. This type of fuel, that are protic solvents such as water, present different physicochemical properties depending upon the amount of biodiesel added to gasoline. As shown in the Nyquist diagrams, the water content of biofuel in the blend is critical for the values of the corrosiveness of ethanol-gasoline blends. This is due both to its role as a solvent for inorganic impurities and its role in the mechanisms of corrosion [15].

Table 3. Comparison between the experimental data for the corrosion system of substratum AA 2124, with 100% regular gasoline and gasoline mixtures of regular and bioethanol at 5%, 10% and 20% percentage.

	R_Ω Ω cm^2	CPE_1 $\mu F\ cm^{-2}\ s^{-(1-\alpha1)}$	α_1	R_1 $10^3 \Omega$ cm^2	CPE_2 $\mu F\ cm^{-2}\ s^{-(1-\alpha2)}$	α_2	R_2 $10^6 \Omega$ cm^2
gasoline	69.28 (0.3%)	29.56 (2.1%)	0.88 (0.2%)	1484 (4%)	146.35 (3%)	0.93 (0.4%)	3.55 (2%)
5%	64.51 (0.3%)	25.44 (1.9%)	0.89 (0.3%)	245 (2%)	112.11 (4%)	0.90 (0.3%)	2.56 (2%)
10%	55.56(0.5%)	12.78 (2.3%)	0.85 (0.3%)	122 (3%)	82.18 (2,6%)	0.58 (0.5%)	0.46(3%)
20%	66.15 (0.5%)	3.45 (3.1%)	0.74 (0.7%)	5.05 (3%)	31.44(1,3%)	0.55 (3.1%)	0.19 (4%)

The α values (table 3), correspond to the exponential coefficient of the phase angle shifting (π/2); the α values for substrata to the CPE at high frequencies values are in the range of 0.74 and 0.89, indicating that surface roughness generates a charge distribution, for CPE at low frequencies shows a α of 0.55 for the bioethanol at 20% and 0.58 for bioethanol at 10%, indicating that migration and diffusion of species are present. For bioethanol at 5% and regular gasoline are present α values of 0.90 and 0.93, generating density distribution of water carries, i.e. a double layer with a complex structure. The data of total impedance better known as the sum of the resistances R_1+R_2 are increasing to the decreasing of the bioethanol percentage (table 3). Moreover, it is observed for the bioethanol at 5% and regular gasoline are much higher than those found in 10% of bioethanol and 20%.
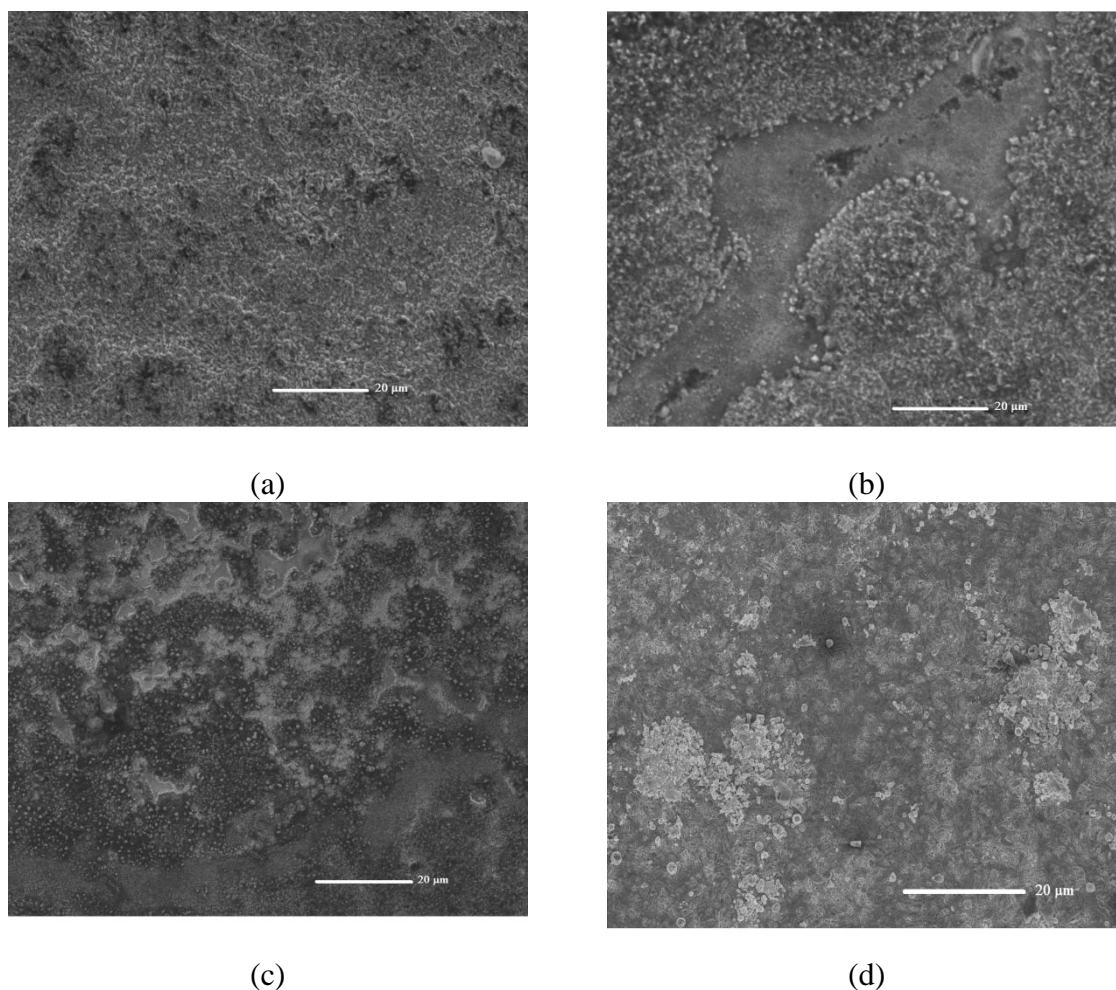
3.3 Microstructural evaluation

(a)   (b)

(c)   (d)

Figure 4. SEM micrograph for aluminum samples (AA2124). a) bioethanol at 20% b) bioethanol at 10%, c) bioethanol at 5%, d) Regular gasoline.

In the figure 4 is observed the sweep electronic microscopy obtained over the surfaces of the AA2124 alloys, after they had been subjected to electrochemical evaluation process. It can be observe

in all the samples a film which presents a corrosion layer, corresponding to an aluminum oxide, this film can be obtain due to accelerated process generating with the polarization curves. The corrosion products formed over the Al alloys surfaces are formed by layers where there are variations in the concentration of oxygen as well as Al, furthermore the Cu and Mg content increases, if is in the internal layer. In the figure 4b (10% of bioethanol), it can be observed the concentration variations so as the oxygen and the aluminum, three layers are distinguished as is mention; it is observed a difference in the texture at the central part. The water presence in the mixture affects the corrosion mechanisms of aluminum alloys.High susceptibility has found in water presence and organic acids in the bioethanol and gasoline mixture (figures 4a, 4b and 4c), with general or superficial corrosion inasmuch as hydroxide is formed as the main corrosion product. The resistance increase is attributed to the non-presence of bioethanol, since is observed in the figure 4a, the aluminum hydroxide formation over the surface can block the corrosion process. It is observed over the surface that is covered by an oxide/hydroxide film of a few nanometers (part of the surface). In the figures 4a, 4b, 4c and 4d are localized corrosion sporadically, but this is related with the presence of the alloys with gasoline, since for the mixture at 20% is not evident this corrosion form.

In other investigations have been carried out with other types of materials such as carbon steel API 5LX-65, using as variable: water content, the presence of chlorides, and corrosion inhibitors, in particular, dissolved oxygen, generate the existence of galvanic couples [16-17]. They also noted that an increase in water content caused a change in the type of corrosion, stress corrosion happening to pitting. They concluded that the probability of occurrence of the phenomenon of stress corrosion cracking in the materials tested, the content depends intimately chlorides present in the commercial ethanol. Other authors studied in detail the mechanism of corrosion of carbon steel in ethanol [18].

4. CONCLUSIONS

The electrochemical techniques allow verifying that the wear velocities of the AA 2124 alloy are directly related with the increase of bioethanol content in the mixture, nevertheless the higher amount of mixture 20% bioethanol gasoline, generates an inferior corrosion velocity of 0.059 µmy, indicating that has good corrosion resistance and can use for applications such as gasoline engines. In the electrochemical impedance spectroscopy diagrams is obtained two layers, one that is related among the aluminum hydroxide layer, which for the 10% and 20% mixtures of bioethanol is obtained diffusion process, they generate the increase of the wear. The other layer is related with the substratum and the adherent alumina layer.

The corrosion products present three kinds of films; one formed with higher oxygen content, the other presents hydroxide and its alumina content is greater. It was found that the corrosion type is general in as much as the presence of aluminum hydroxides reduces the localized corrosion susceptibility.

References

1. C.E. Goering, *Transactions of the American Society of Agricultural Engineers (ASAE)*, 25 (1982) 1472.
2. H.K. Adli, W.M. Khairul, and H. Salleh, *Int. J. Electrochem. Sci*, 7 (2012) 499.
3. R. Altin, S. Cetinkaya and H.S. Yucesu, *Energy Convers Manage*, 42 (2001) 529.
4. L. Louise, S. Sousa, L. Izabelly, L. Lucena and A.N. Fernandes, *Fuel Processing Technology*, 91 (2010) 194.
5. B.K. Barnwal and M.P. Sharma, *Renew Sustain Energy Rev*, 9 (2005) 363.
6. Z.A. Jarjes, M.R. Samian and S.A. Ghani, *Int. J. Electrochem. Sci*, 6 (2011) 1317.
7. M. Gauder, S. Graeff-Hönninger and W. Claupein, Applied Energy, 88 (2011) 672.
8. L. Hernández and V. Kafarov, *Int. J. Hydrogen Energy*, 34 (2009) 7041.
9. D. Krajnc and P. Glavič, *Chemical Engineering Research and Design*, 87 (2009) 1217.
10. S. Kim and B.E. Dale, *Biomass and Bioenergy*, 26 (2004) 361.
11. D.Y. Peña-Ballesteros, H.A. Estupiñán-Durán and C. Vásquez-Quintero, Evaluación de la corrosión de un duraluminio en mezclas de gasolina y bioetanol. *Ing. Univ*, 16 (2012) 9.
12. L. Díaz-Ballote, J.F. López-Sansores, L. Maldonado-López and L.F. Garfias-Mesias, *Electrochem. Commun.*, 11 (2009) 41.
13. F. Mansfield, *J. Chem. Soc*. 120 (1973) 188.
14. V. B. Singh y V. K. Singh, *Mater. Trans*. 32 (1991) 251.
15. J. Banas, *Electrochem. Acta* 32 (1987) 871.
16. N. Sridhar, K. Price, J. Buckingham y J. Dante, *Corrosion* 62 (2006), 687.
17. X. Lou, D. Yang y P. M. Singh, *Corrosion* 65 (2009) 785.
18. X. Lou, D. Yang y P. M. Singh, *J. Electrochem.* 157 (2010) 86.